Neuroprotective effects of anti-high mobility group box-1 monoclonal antibody against methamphetamine-induced dopaminergic neurotoxicity

Kaori Masai[1], Keita Kuroda[1], Nami Isooka[1], Ryo Kikuoka[1], Shinki Murakami[1], Sunao Kamimai[2], Dengli Wang[3], Keyue Liu[3], Ikuko Miyazaki[1], Masahiro Nishibori[3] and Masato Asanuma[1, *]

[1]Department of Medical Neurobiology, Okayama University Graduate School of Medicine, Dentistry and Pharmaceutical Sciences, Okayama 700-8558, Japan.
[2]Department of Medical Neurobiology, Okayama University Medical School, Okayama 700-8558, Japan
[3]Department of Pharmacology, Okayama University Graduate School of Medicine, Dentistry and Pharmaceutical Sciences, Okayama 700-8558, Japan

*Corresponding author:
Masato Asanuma, M.D., Ph.D.,
Department of Medical Neurobiology, Okayama University Graduate School of Medicine, Dentistry and Pharmaceutical Sciences
2-5-1 Shikata-cho, Kita-ku, Okayama 700-8558, Japan
Tel: +81-86-235-7096
Fax: +81-86-235-7103
E-mail address: asachan@cc.okayama-u.ac.jp

Abstract

High mobility group box-1 (HMGB1) is a ubiquitous non-histone nuclear protein that plays a key role as a transcriptional activator, with its extracellular release provoking inflammation. Inflammatory responses are essential in methamphetamine (METH)-induced acute dopaminergic neurotoxicity. In the present study, we examined the effects of neutralizing anti-HMGB1 monoclonal antibody (mAb) on METH-induced dopaminergic neurotoxicity in mice. BALB/c mice received a single intravenous administration of anti-HMGB1 mAb prior to intraperitoneal injections of METH (4 mg/kg×2, at 2-h intervals). METH injections induced hyperthermia, an increase in plasma HMGB1 concentration, degeneration of dopaminergic nerve terminals, accumulation of microglia and extracellular release of neuronal HMGB1 in the striatum. These METH-induced changes were significantly inhibited by intravenous administration of anti-HMGB1 mAb. In contrast, blood-brain barrier disruption occurred by METH injetions was not suppressed. Our findings demonstrated the neuroprotective effects of anti-HMGB1 mAb against METH-induced dopaminergic neurotoxicity, suggesting that HMGB1 could play an initially important role in METH toxicity.

Keywords: methamphetamine; dopamine neuron; high mobility group box-1; hyperthermia; inflammation; neurotoxicity

Introduction

Methamphetamine (METH), a drug of abuse, causes degeneration of striatal dopaminergic nerve terminals. Various neurotoxic factors have been proposed as causes of METH-induced neurotoxicity, including reactive oxygen species (ROS), reactive nitrogen species, dopamine (DA) quinone formation, glutamate release, hyperthermia, and proapoptotic molecular events (Ali et al. 1994; Cadet and Brannock 1998; Cadet et al. 2003; Miyazaki et al. 2006). In addition, a number of studies have indicated that neuroinflammatory processes with microglial activation play an important role in METH toxicity (Asanuma et al. 2003; Bowyer et al. 2008; Fantegrossi et al. 2008; Granado et al. 2011; Kays and Yamamoto 2019; Krasnova and Cadet 2009; Loftis and Janowsky 2014; Raineri et al. 2012; Thomas and Kuhn 2005; Thomas et al. 2004). Reportedly, METH-induced dopaminergic neurotoxicity with microglial activation and accumulation was attenuated by the treatment with non-steroidal anti-inflammatory drugs (NSAIDs) (Asanuma et al. 2004; Asanuma et al. 2003; Tsuji et al. 2009), especially indomethacin and ibuprofen which act as agonists for peroxisome proliferator-activated receptor γ (PPARγ), and intrinsic PPARγ agonist PGJ2 (Asanuma et al. 2004; Tsuji et al. 2009), and with minocycline which prevents microglia activation (Zhang et al. 2006) or in IL-6 knockout mice (Ladenheim et al. 2000).

High mobility group box-1 (HMGB1) binds DNA in the nuclei as a transcriptional regulator. Extracellular HMGB1, secreted not only from any type of apoptotic or necrotic cells but also from various inflammatory damaged cells, functions as damage-associated molecular patterns (DAMPs), and as an activator of proinflammatory cytokines and pathogen-associated molecular patterns (PAMPs), to exacerbate inflammation through binding to receptor for advanced glycation end products (RAGE) and toll-like receptors (TLR2/TLR4) (Bell et al. 2006; Frank et al. 2015; Kwak et al. 2020; Muhammad et al. 2008; Park et al. 2004; Paudel et al. 2018; Qiu et al. 2008). It has been demonstrated that extracellular HMGB1 is significantly increased in the acute phase of the post-ischemic brain and activates microglia, resulting in delayed neuroinflammation (Kim et al. 2008; Kim et al. 2006). Furthermore, chronic dopaminergic neurodegeneration in the mesencephalon was caused by HMGB1 release, which promoted microglial activation via macrophage antigen 1, resulting in the release of cytokines, including the nuclear factor κB (NF-κB) pathway, and nicotinamide adenine dinucleotide phosphate sodium salt hydrate (NADPH) oxidase (Gao et al. 2011). Moreover, HMGB1 is thought to be neuroinflammatory pathogenesis of various neurological diseases (Paudel et al. 2018), including ischemic brain infarction (Kim et al. 2008; Liu et al. 2007; Zhang et al. 2011), cerebral hemorrhage (Haruma et al. 2016; Wang et

al. 2017), traumatic brain injury (Okuma et al. 2012), dopaminergic neurodegeneration in Parkinson's disease (Sasaki et al. 2016), convulsion (Fu et al. 2017), and neuropathic pain (Nakamura et al. 2013; Shibasaki et al. 2010; Zhang et al. 2016). We previously reported that the anti-HMGB1 monoclonal antibody (mAb) inhibited microglial activation and blood-brain barrier (BBB) disruption to ameliorate infarction after transient brain ischemia (Liu et al. 2007; Zhang et al. 2011), and that the Ab also showed therapeutic effects to suppress traumatic brain injury-induced brain edema and inflammatory response (Okuma et al. 2012). Furthermore, our previous study revealed that anti-HMGB1 antibody inhibits microglial activation, neuroinflammation, dopaminergic neurodegeneration, and motor deficits in a rat model of Parkinson's disease (Sasaki et al. 2016). Thus, we have demonstrated the neuroprotective effects of anti-HMGB1 mAb against various HMGB1-related neuronal damages (Fu et al. 2017; Haruma et al. 2016; Liu et al. 2007; Nakamura et al. 2013; Okuma et al. 2012; Sasaki et al. 2016; Wang et al. 2017; Zhang et al. 2016; Zhang et al. 2011), suggesting that an anti-HMGB1 antibody could be a candidate drug for neuroinflammation in diverse diseases. Herein, we examined whether anti-HMGB1 mAb could protect dopaminergic neurons against METH toxicity.

Materials and Methods

Animal and Reagents

All animal procedures described in our experiments were in strict accordance with the NIH Guide for the Care and Use of Experimental Animals and the Policy on the Care and Use of the Laboratory Animals of Okayama University and were approved by the Animal Care and Use Committee of Okayama University (approval reference number OKU-2017131 and OKU-2020008, approved on April 1, 2017, and April 1, 2020, respectively). Additionally, special care was taken to minimize the number of animals used. Male BALB/c mice (9 weeks old; Charles River Japan Inc., Yokohama, Japan) were housed in a temperature- and humidity-controlled room, with a 12-h light/dark cycle and free access to food and water *ad libitum*. METH hydrochloride (Dainippon Pharmaceutical, Osaka, Japan) was diluted using saline.

Drug Administration and Rectal Temperature Measurement

Under anesthesia by inhalation of isoflurane, BALB/c mice were intravenously administered anti-HMGB1 mAb (#10-22, rat IgG2a subclass, 1 mg/kg), class-matched control IgG (rat anti-keyhole limpet hemocyanin mAb), or phosphate-buffered saline

(PBS), followed by repeated METH injections (4 mg/kg×2, i.p. with 2-h interval) or the same volume of saline. The most commonly used regimen (5 mg/kg×4, i.p. with 2-h interval) for the experiments on METH neurotoxicity are lethal in CD-1 (ICR) strain supplied Japanese companies. It is confirmed that multiple lower dose (4 mg/kg) using BALB/c strain brings similar METH-induced dopaminergic neurotoxicity in the striatum (Asanuma et al. 2004; Asanuma et al. 2003; Hozumi et al. 2008). Rectal temperature was recorded just before or every 1 h after the first METH injection for up to 5 h using a monitoring thermometer (Bio Research Center, Osaka).

Measurement of HMGB1 in Plasma

To determine the HMGB1 level in plasma samples, blood samples (2 ml) were collected using EDTA to prevent hemolysis via the heart under deep anesthesia with sodium pentobarbital (100 mg/kg, i.p.) 6 h after the first METH injection. Then, blood samples were centrifuged at 3,000 rpm for 10 min at 4°C. The supernatant was used for measurement of HMGB1 using an enzyme-linked immunosorbent assay kit (Shino-Test Co, Sagamihara, Japan) according to the manufacturer's protocol (Zhang et al. 2011).

Immunohistochemistry

Three days after the last METH injection, mice were transcardially perfused with saline followed by a fixative containing 4% paraformaldehyde in 0.1M phosphate buffer (PB: pH 7.4) under deep pentobarbital anesthesia. After perfusion, the brains were quickly removed from the skull, post-fixed for 24 h using a fixative containing 4% paraformaldehyde in 0.1M PB (pH 7.4), and then paraffin-embedded, or cryoprotected in 15% sucrose in PB for approximately 48 h, followed by snap freezing with powdered dry ice. Paraffin-embedded brains were cut coronally at 4-μm thickness, and frozen brains were cut coronally on a cryostat at levels containing the mid-striatum (+0.6~+1.0 mm from the bregma) at 20-μm thickness.

To evaluate the degeneration of dopaminergic nerve terminals and BBB disruption, immunostaining of dopamine transporter (DAT) and extravascular albumin in the mid-striatum was performed by standard immunohistochemistry (Asanuma and Cadet 1998; Asanuma et al. 2003). The frozen sections were soaked in 10 mM PBS containing 0.2% Triton X-100 (PBST) for 1 h, followed by incubation in 0.5% H_2O_2 in PBST for 30 min at room temperature (RT). After washing with PBST (3 × 10 min), the brain slices were blocked with 1% normal rabbit serum in PBST for 30 min, and then incubated with

rat anti-DAT monoclonal antibody (diluted 1:1,000 in PBST; Millipore, Temecula, CA, USA) or goat anti-albumin polyclonal antibody (diluted 1:250 in PBST; BETHYL, Montgomery, TX, USA) for 16 h at 4°C. After washing in PBST (5 × 5 min), slices were reacted with rabbit anti-rat IgG or rabbit anti-goat IgG biotinylated secondary antibody (diluted 1:1,000 in PBST: Vector Laboratories, Inc., Burlingame, CA) for 1.5 h at RT. Following washes using PBST (3 × 10 min), the sections were incubated with the avidin-biotin-peroxidase complex (diluted 1:2,000 in PBST) for 1 h. Immunopositive cells were visualized using 3,3'-diaminobenzidine tetrahydrochloride, nickel ammonium sulfate, and H_2O_2. The relative density of DAT-positive or albumin-positive signals in the mid-striatum was semi-quantified using a microscope at a magnification of 40× and a computer-based image analysis system (Image J 1.44k, National Institutes of Health, Bethesda, MD, USA). Each side of the mid-striatum on the digitized image was separately outlined using a screen cursor driven by a hand-held mouse, and relative density of DAT signals in the mid-striatum was measured by subtracting the background density in the lateral ventricle of each slice (Asanuma and Cadet 1998). Relative density of albumin signals was measured by subtracting the background density in the cortex and non-specific signal in striatal white-matter tracts of each slice.

For fluorescence immunostaining of ionized calcium-binding adaptor molecule 1 (Iba1), the striatal frozen sections were incubated in 1% normal goat serum for 30 min at RT, and then reacted with rabbit anti-Iba1 polyclonal antibody (diluted 1:1,000 in PBST; Wako Pure Chemical Industries, Osaka) for 18 h at 4°C. After washing, the sections were incubated with goat anti-rabbit IgG conjugated to Alexa Fluor 488 (1:1,000, Molecular Probes, Eugene, OR, USA) for 2 h at RT, and then counterstained with Hoechst 33342 nuclear stain. Iba1-positive signals were analyzed under a fluorescence microscope (Olympus BX53, Tokyo, Japan) and cellSens software imaging system (Olympus) using a mercury lamp through a 470-490 nm band-pass filter to excite Alexa Fluor 488. The light emitted from Alexa Fluor 488 was collected through a 510-550 nm band-pass filter. Iba1-immunopositive microglial cells in the mid-striatum were manually counted using a microscope at a magnification of 200× with a superimposed grid (Asanuma and Cadet 1998; Asanuma et al. 2003). Counting was performed blindly.

To explore localization and release of HMGB1, double staining of HMGB1 and NeuN or glutamine synthetase (GS) was performed. Paraffin sections were deparaffinized in xylene, rehydrated in graded ethanol solutions, and subjected to antigen retrieval by autoclave in 10 mM sodium citrate (pH 6.0) for 5 min at 121°C. After return to RT, the

sections were incubated in 1% normal donkey serum for 30 min at RT, and then reacted with rabbit anti-HMGB1 polyclonal antibody (diluted 1:500 in PBST; Abcam, Cambridge, UK) and mouse anti-NeuN monoclonal antibody (diluted 1:1,000 in PBST; Millipore) or mouse anti-GS monoclonal antibody (diluted 1:1000 in PBST; Millipore) for 18 h at 4°C. After washing, the sections were incubated with donkey anti-rabbit IgG conjugated to Alexa Fluor 488 and donkey anti-mouse IgG conjugated to Alexa Fluor 594 (1:1,000, Molecular Probes, Eugene, OR, USA) for 2 h at RT, and then counterstained with Hoechst dye. Localization of HMGB1 and NeuN or GS signals was confirmed by confocal laser-scanning microscopy (LSM780; ZEISS, Oberkochen, Germany). Light emitted from Hoechst 33342, Alexa Fluor 488 or Alexa Fluor 594 was collected through a 420-470 nm band-pass filter, a 500-550 nm band-pass filter, or a 570-640 nm band-pass filter, respectively. Images were taken at a magnification of 400 × and recorded using the Windows-based LSM program (ZEISS).

Western Blot Analysis

Mice were sacrificed 2 h after the second METH injection. Nuclear lysates from the striatum were extracted using NE-PER Nuclear and Cytoplasmic Extraction Reagents (Thermo Fisher Scientific Inc., Rockford, IL, USA) according to the protocol provided with the kit. Western blot analysis was performed as described previously (Miyazaki et al. 2013). In brief, proteins were separated on 10% SDS polyacrylamide gels (Bio-Rad, Hercules, CA) at 20 mA/membrane for 60 min and electrophoretically transferred to polyvinylidene difluoride membranes (Immobilon-P, Merck Millipore, Billerica, MA, USA). The membranes were pre-incubated with a blocking buffer (Block-Ace; DS Biopharma Medical, Tokyo, Japan), and incubated with rabbit anti-NF-κB p65 (1:2000; Abcam) or goat anti-Lamin B (1:200; Santa Cruz Biotechnology, Santa Cruz, CA) polyclonal antibodies. After washing with 20 mM Tris-buffered saline containing 0.1% Tween 20 (Wako, Tokyo), the blots were incubated with the corresponding horseradish peroxidase-conjugated secondary antibodies. Signals were visualized via chemiluminescence using an ELC Western blotting detection system (GE Healthcare, Buckinghamshire, UK). Images were obtained and quantified using a FUJIFILM Luminescent Image Analyzer LAS-3000 (FUJIFILM, Tokyo) and Multi Gauge (v 3.0) software. For quantitative analysis, the signal ratio of NF-κB p65 (relative chemiluminescence unit) to that of constitutively expressed Lamin B protein was calculated for normalization of loading and transfer artifacts. For western blot analysis, the nuclear fraction with low concentration was excluded prior to electrophoresis.

Statistical Analysis

Each value is expressed as the mean ± standard error of the mean (SEM). Statistical analyses for indices were performed using one-way ANOVA or two-way ANOVA (for data of rectal temperature) followed by Fisher's PLSD *post hoc* test. A p-value of less than 0.05 was considered a significant difference.

Results

Effects of Anti-HMGB1 mAb on METH-Induced Hyperthermia and Elevation of Plasma HMGB1

Repeated METH injections (4 mg/kg×2, i.p. at 2-h intervals) significantly increased rectal temperature (hyperthermia) in BALB/c mice 1 h after the second METH injection (3 h after the first METH injection) (group × time, F (25, 150) = 1.715, $p < 0.05$, two-way ANOVA) (Fig. 1B). Intravenous administration of anti-HMGB1 mAb (1 mg/kg), but not control IgG, inhibited METH-induced hyperthermia at 2 h after the second METH injection (vs. METH + PBS-treated group, $p < 0.001$, two-way ANOVA) (Fig. 1B). The plasma HMGB1 concentration was significantly increased 6 h after the last METH injection. Anti-HMGB1 mAb injection inhibited the elevation of plasma HMGB1 levels (Fig. 1C).

Neuroprotective Effects of Anti-HMGB mAb Against METH-Induced Degeneration of Dopaminergic Nerve Terminals in the Mouse Striatum

Repeated METH injections reduced DAT-positive signals in the mid-striatum, especially in the laterodorsal legion. Intravenous injection of anti-HMGB1 mAb (1 mg/kg), but not PBS or control IgG, completely inhibited the METH-induced reduction of DAT signals in the mid-striatum (Fig. 2A, B).

Effects of Anti-HMGB1 mAb on the METH-Induced Accumulation of Iba1-Positive Microglial Cells in the Mouse Striatum

Morphologically, microglial cells were altered to hypertrophic and amoeboid in shape after METH injections (Fig. 3B). Three days after repeated METH injections, the number of Iba1-immunoreactive microglial cells was significantly increased in the laterodorsal region of the mid-striatum. The METH-induced microglial accumulation in the mid-striatum was significantly attenuated following the administration of anti-HMGB1 mAb, but not by control IgG (Fig. 3A-C).

Effects of Anti-HMGB1 mAb Against METH-Induced BBB Disruption

Several studies reported that METH-induced hyperthermia could induce the breakdown of the BBB (Bowyer and Ali 2006; Kiyatkin et al. 2007). Immunohistochemical study for albumin demonstrated that METH injections caused significant elevation of albumin immunoreactivity in the striatum, i.e. the influx of albumin into the cerebral parenchyma by BBB impairment. Anti-HMGB1 mAb administration did not inhibit the leakage of albumin. (Fig. 4A, B).

Effects of Anti-HMGB1 mAb on the METH-Induced HMGB1 Translocation

Previous studies have shown that HMGB1 is constitutively expressed in the nuclei of neurons, and translocated to the cytoplasm, followed by the release from damaged cells in neuroinflammatory conditions (Fang et al. 2012; Tang et al. 2011). To assess the dynamics of HMGB1 in the striatum of METH-treated mice, we performed double immunostaining of HMGB1 and NeuN, a marker of the neuronal nucleus, or GS, a marker for astrocyte. METH injection increased HMGB1 expression in the neuronal nuclei and induced extracellular signals of HMGB1, suggesting the protein release into the extracellular space. Anti-HMGB1 mAb treatment inhibited METH-induced upregulation of HMGB1 and translocation (Fig. 5). In contrast, while HMGB1 was also localized in the astrocyte nuclei, METH did not increase the expression (Fig. 6).

Changes in Nuclear NF-κB Expression in the Striata of Mice after Injections of METH with/without Anti-HMGB1 mAb

Reportedly, METH injections induce NF-κB nuclear translocation, which can cause inflammation (Asanuma and Cadet 1998; Asanuma et al. 2002). Therefore, we examined changes in nuclear NF-κB p65 expression in the striata of mice by western blot analysis. Two hours after METH injections, we observed an increasing tendency, but not a significant increase, of nuclear translocation of NF-κB expression, which was inhibited by anti-HMGB1 mAb (data not shown).

Discussion

Various mechanisms of METH-induced neurotoxicity have been hypothesized. METH induces excessive DA release from synaptic vesicles, which causes ROS and DA quinone production by DA auto-oxidation (De Vito and Wagner 1989; Kita et al. 2009; Kita et al.

2000; Miyazaki et al. 2006). Furthermore, it has been reported that METH impairs mitochondrial ATP production (Burrows et al. 2000a; Thrash-Williams et al. 2016). METH-induced excessive glutamate release leads to neuronal excitotoxicity and nitric oxide synthase activation (Abekawa et al. 1994; Deng and Cadet 1999). In addition, METH induces the activation of astrocytes and microglia, which cause proinflammatory cytokine production (Loftis and Janowsky 2014). BBB disruption has been observed in METH-injected animals, which is occurred by decrease in tight junction complex and increase in matrix-degrading proteinases (Conant et al. 2004; Mahajan et al. 2008). Along with these observations, multiple mechanisms interact with each other and promote METH neurotoxicity (Kousik et al. 2012; Krasnova and Cadet 2009).

Furthermore, hyperthermia is considered to be associated with dopaminergic neuronal damage; however, it is controversial whether hyperthermia is involved in METH neurotoxicity (Bowyer et al. 1994). A previous study has shown that METH direct injection into the striatum did not cause hyperthermia, but it increased extracellular DA levels (Burrows et al. 2000b). Our previous study found that intracerebroventricular interferon-γ (IFN-γ) inhibits METH-induced striatal DAT loss, but not hyperthermia; in contrast, intraperitoneal IFN-γ suppressed both of them (Hozumi et al. 2008). Edaravone, known as a free radical scavenger, protected dopaminergic neurons from METH toxicity, although it failed to inhibit hyperthermia and microglial activation (Kawasaki et al. 2006). Additionally, repeated injections of ibuprofen, a NSAID and a PPARγ agonist, also failed to demonstrate an effect on METH-induced hyperthermia; while ibuprofen attenuated METH-induced reduction of DAT, upregulation of cyclooxygenase expression, and accumulation of activated microglia in the striatum (Tsuji et al. 2009). These findings suggest that METH-induced hyperthermia could be involved upper stream of the METH toxicity cascade. Several mechanisms of METH-induced hyperthermia have been suggested: acceleration of the central nervous system (CNS) metabolism and skeletal muscle activity by stimulating catecholamine release (Makisumi et al. 1998; Matsumoto et al. 2014), inhibition of peripheral heat dissipation by vasoconstriction (Gordon et al. 1991), increased IL-1β in the hypothalamus (Bowyer et al. 1994; Yamaguchi et al. 1991), and interaction of hypothalamic sigma receptors (Seminerio et al. 2012).

METH-induced hyperthermia and decrease of tight junctions could result in the impairment of the BBB (Bowyer and Ali 2006; Kiyatkin et al. 2007), which can promote a vicious circle of neurotoxicity. Reportedly, peripheral HMGB1 is involved in the molecular mechanisms of BBB disruption. Festoff *et al.* have demonstrated that HMGB1 impaired BBB

integrity by downregulating zonula occludens protein-1 (ZO-1) expression (Festoff et al. 2016). The present study demonstrated that anti-HMGB1 mAb treatment suppressed hyperthermia but not BBB breakdown. The findings indicate that anti-HMGB1 mAb could not break the vicious cycle of hyperthermia and BBB disruption. These resulting data suggest two possible mechanisms of anti-HMGB1 mAb. First, the Ab could transfer from peripheral blood to CNS via disrupted BBB. Translocated anti-HMGB1 mAb might suppress METH-induced neuroinflammation in the hypothalamus to inhibit hyperthermia. Second, neutralization of peripheral HMGB1 by the antibody could inhibit hyperthermia derived from METH-induced vasoconstriction and skeletal muscle activity disorder.

The present study showed inhibiting effects of anti-HMGB1 mAb against loss of dopaminergic nerve terminals, microglia activation, and release of HMGB1 from the neuronal nuclei. Previous studies demonstrated the involvement of inflammatory molecular and cellular events in METH-induced dopaminergic neurotoxicity (Papageorgiou et al. 2019), namely elevation of inflammation-inducible transcription factors such as NF-κB (Asanuma and Cadet 1998; Asanuma et al. 2002). It has also been reported that METH upregulates the expression of HMGB1 in parallel with IL-1β in the striatum and that Box A, which is an HMGB1 antagonist at Toll-like receptor 4 (TLR4), blocks its neuroinflammatory effects in the nucleus accumbens, ventral tegmental area and prefrontal cortex, suggesting that HMGB1 could mediate METH-induced neuroinflammation by stimulating innate immune cells (Frank et al. 2016). An *in vitro* study demonstrated that METH exposure increased expression of ERK MAP kinase, NF-κB p65 nuclear translocation and HMGB1 expression in astroglial C6 cells (Zhang et al. 2015). Interestingly, HMGB1 translocation to cytosol is mainly observed at neurons, by contrast, also at a small number of microglia and few astrocytes in the early phase of subarachnoid hemorrhage model rat (Sun et al. 2017). However, it remains unclear which cells are main source of HMGB1 in METH treatment *in vivo*. Our study revealed the increase of HMGB1 production and release from neuronal nuclei, but not astrocytes in the striatum of METH-treated mice. Besides, previous reports demonstrated that METH treatment activated astrocytes and microglia (Asanuma et al. 2003; Friend and Keefe 2013; Loftis and Janowsky 2014). Frank *et al.* also presented that direct treatment with METH did not increase release of pro-inflammatory cytokines from primary culture of microglia (Frank et al. 2016). Taken together with these observations, it is suggested that HMGB1 released from neurons after METH exposure might initially activate neighbor astrocytes and microglia, and consequently promote neuroinflammation. METH provokes a microglial inflammatory response by activating the TLR4 signaling pathway, including IκB kinase, NF-κB, and

interferon regulatory factor 3 in cultured microglial cells (Vargas et al. 2020). In neutrophils, nuclear translocation of NF-κB is upregulated after HMGB1 treatment (Park et al. 2004). In the brains of patients with intractable epilepsy, cytoplasmic HMGB1 and nuclear NF-κB were significantly increased in pyramidal neurons and glial cells when compared with the control group, in which HMGB1 is mostly detected in the nuclei. Furthermore, increased levels of reactive microglia and elevation of HMGB1 and NF-κB expression levels in brain tissues were also observed (Shi et al. 2018). However, there was no significant alteration in the nuclear translocation of NF-κB in the striatum of our METH-injected mice. In our study, BALB/c mice received intraperitoneal METH injections twice to assess the protective effects of anti-HMGB1 mAb against acute neurotoxicity, considering the duration of drug activity. Therefore, the toxicity may be insufficient to cause apparent NF-κB translocation.

The neuroprotective effects of anti-HMGB1 mAb on METH neurotoxicity may be based on suppressing METH-induced neuroinflammation by translocated Ab into the brain and/or its quenching peripheral circulating HMGB1 to supress invasion of HMGB1 or inflammatory molecules into the brain. Further examination by intrastriatal injection of the anti-HMGB1 mAb will be required to clarify the minute mechanism of neuroprotection.

Conclusion

In summary, our study demonstrated that the intravenous administration of anti-HMGB1 mAb neutralized peripheral HMGB1, resulting in suppression of METH-induced hyperthermia, microglial activation, release of HMGB1 from the neuronal nuclei in the CNS, and dopaminergic neurotoxicity in the striatum. These results suggest that HMGB1 could play a pivotal role in METH neurotoxicity and proposed anti-HMGB1 mAb as a novel approach to prevent METH toxicity.

Acknowledgements

The authors would like to thank Dr. Yu Okuma for his technical assistance with measuring plasma HMGB1 level.

Declarations

Funding

This work was supported by Health and Labour Sciences Research Grants for Research on Regulatory Science of Pharmaceuticals and Medical Devices (H30-IYAKU-IPPAN-004 to M.A.) from the Japanese Ministry of Health, Labour and Welfare, and by Grants-in-Aid for

Scientific Research (C) (KAKENHI #25461279 to I.M.) and Grants-in-Aid for Scientific Research (B) (KAKENHI #19H03408 to M.N.) from the Japan Society for the Promotion of Science, by a Grant-in-Aid for Scientific Research on Innovative Areas "Brain Environment" (KAKENHI #24111533 to M.A.) from the Japanese Ministry of Education, Culture, Sports, Science, and Technology, and by a Research Grant from the Okayama Medical Foundation (to I.M.).

Conflict of interest

All authors have no actual or potential conflicts of interest, including financial, personal, or other relationships with other people or organizations.

Author's contributions

M.A. and I.M. designed the experiment. K.M., K.K., N.I., R.K., S.M., D.W., K.L., S.K., and I.M. performed experiment and data analysis. K.M. and M.A. wrote the main manuscript text and prepared all figures. M.N. and M.A. supervised this study. All authors read and approved the manuscript.

Ethics approval

All animal procedures described in our experiments were in strict accordance with the NIH Guide for the Care and Use of Experimental Animals and the Policy on the Care and Use of the Laboratory Animals of Okayama University and were approved by the Animal Care and Use Committee of Okayama University (approval reference number OKU-2017131 and OKU-2020008, approved on April 1, 2017, and April 1, 2020, respectively). All experiments were conducted in compliance with the ARRIVE guidelines.

Abbreviations

ANOVA, analysis of variance; BBB, blood-brain barrier; DAMP, damage-associated-molecular-pattern; DAT, dopamine transporter; DMSO, dimethylsulphoxide; GFAP, glial fibrillary acidic protein; HMGB1, high mobility group box-1; Iba1, ionized calcium binding adaptor molecule 1; IFN-γ, interferon-γ; IL, interneukin; mAb, monoclonal antibody; METH, methamphetamine; NF-κB, nuclear factor κB; NSAID, nonsteroidal anti-inflammatory drugs; PPARγ, peroxisome proliferator-activated receptor γ; PB, phosphate buffer; PBS-T, phosphate buffered saline

with 0.2% Triton X-100; RAGE, receptor for advanced glycation end products; ROS, reactive oxygen species; RT, room temperature; TH, tyrosine hydroxylase; TLR, toll-like receptor

References

Abekawa T, Ohmori T, Koyama T (1994) Effects of repeated administration of a high dose of methamphetamine on dopamine and glutamate release in rat striatum and nucleus accumbens. Brain Res 643:276-281. https://doi.org/10.1016/0006-8993(94)90033-7

Ali SF, Newport GD, Holson RR, Slikker W, Jr., Bowyer JF (1994) Low environmental temperatures or pharmacologic agents that produce hypothermia decrease methamphetamine neurotoxicity in mice. Brain Res 658:33-38. https://doi.org/10.1016/s0006-8993(09)90007-5

Asanuma M, Cadet JL (1998) Methamphetamine-induced increase in striatal NF-kB DNA-binding activity is attenuated in superoxide dismutase transgenic mice. Mol Brain Res 60:305-309. https://doi.org/10.1016/s0169-328x(98)00188-0

Asanuma M, Miyazaki I, Higashi Y, Cadet JL, Ogawa N (2002) Methamphetamine-induced increase in striatal p53 DNA-binding activity is attenuated in Cu,Zn-superoxide dismutase transgenic mice. Neurosci Lett 325:191-194. https://doi.org/10.1016/s0304-3940(02)00291-4

Asanuma M, Miyazaki I, Higashi Y, Tsuji T, Ogawa N (2004) Specific gene expression and possible involvement of inflammation in methamphetamine-induced neurotoxicity. Ann NY Acad Sci 1025:69-75. https://doi.org/10.1196/annals.1316.009

Asanuma M, Tsuji T, Miyazaki I, Miyoshi K, Ogawa N (2003) Methamphetamine-induced neurotoxicity in mouse brain is attenuated by ketoprofen, a non-steroidal anti-inflammatory drug. Neurosci Lett 352:13-16. https://doi.org/10.1016/j.neulet.2003.08.015

Bell CW, Jiang W, Reich CF III, Pisetsky DS (2006) The extracellular release of HMGB1 during apoptotic cell death. Am J Physiol Cell Physiol 291:C1318-C1325. https://doi.org/10.1152/ajpcell.00616.2005

Bowyer JF, Ali S (2006) High doses of methamphetamine that cause disruption of the blood-brain barrier in limbic regions produce extensive neuronal degeneration in mouse hippocampus. Synapse 60:521-532. https://doi.org/10.1002/syn.20324

Bowyer JF, Davies DL, Schmued L, Broening HW, Newport GD, Slikker W, Jr., Holson RR (1994) Further studies of the role of hyperthermia in methamphetamine neurotoxicity. J Pharmacol Exp Ther 268:1571-1580

Bowyer JF, Robinson B, Ali S, Schmued LC (2008) Neurotoxic-related changes in tyrosine hydroxylase, microglia, myelin, and the blood-brain barrier in the caudate-putamen

from acute methamphetamine exposure. Synapse 62:193-204. https://doi.org/10.1002/syn.20478

Burrows KB, Gudelsky G, Yamamoto BK (2000a) Rapid and transient inhibition of mitochondrial function following methamphetamine or 3,4-methylenedioxymethamphetamine administration. Eur J Pharmacol 398:11-18. https://doi.org/10.1016/s0014-2999(00)00264-8

Burrows KB, Nixdorf WL, Yamamoto BK (2000b) Central administration of methamphetamine synergizes with metabolic inhibition to deplete striatal monoamines. J Pharmacol Exp Ther 292:853-860

Cadet JL, Brannock C (1998) Free radicals and the pathobiology of brain dopamine systems. Neurochem Int 32:117-131. https://doi.org/10.1016/s0197-0186(97)00031-4

Cadet JL, Jayanthi S, Deng X (2003) Speed kills: cellular and molecular bases of methamphetamine-induced nerve terminal degeneration and neuronal apoptosis FASEB J 17:1775-1788. https://doi.org/10.1096/fj.03-0073rev

Conant K, St Hillaire C, Anderson C, Galey D, Wang J, Nath A (2004) Human immunodeficiency virus type 1 Tat and methamphetamine affect the release and activation of matrix-degrading proteinases. J Neurovirol 10:21-28. https://doi.org/10.1080/13550280490261699

De Vito MJ, Wagner GC (1989) Methamphetamine-induced neuronal damage: a possible role for free radicals. Neuropharmacology 28:1145-1150. https://doi.org/10.1016/0028-3908(89)90130-5

Deng X, Cadet JL (1999) Methamphetamine administration causes overexpression of nNOS in the mouse striatum. Brain Res 851:254-257. https://doi.org/10.1016/s0006-8993(99)02087-9

Fang P, Schachner M, Shen YQ (2012) HMGB1 in development and diseases of the central nervous system. Mol Neurobiol 45:499-506. https://doi.org/10.1007/s12035-012-8264-y

Fantegrossi WE, Ciullo JR, Wakabayashi KT, De La Garza R II, Traynor JR, Woods JH (2008) A comparison of the physiological, behavioral, neurochemical and microglial effects of methamphetamine and 3,4-methylenedioxymethamphetamine in the mouse. Neuroscience 151:533-543. https://doi.org/10.1016/j.neuroscience.2007.11.007

Festoff BW, Sajja RK, van Dreden P, Cucullo L (2016) HMGB1 and thrombin mediate the blood-brain barrier dysfunction acting as biomarkers of neuroinflammation and progression to neurodegeneration in Alzheimer's disease. J Neuroinflammation

13:194. https://doi.org/10.1186/s12974-016-0670-z

Frank MG, Adhikary S, Sobesky JL, Weber MD, Watkins LR, Maier SF (2016) The danger-associated molecular pattern HMGB1 mediates the neuroinflammatory effects of methamphetamine. Brain Behav Immun 51:99-108. https://doi.org/10.1016/j.bbi.2015.08.001

Frank MG, Weber MD, Watkins LR, Maier SF (2015) Stress sounds the alarmin: The role of the danger-associated molecular pattern HMGB1 in stress-induced neuroinflammatory priming. Brain Behav Immun 48:1-7. https://doi.org/10.1016/j.bbi.2015.03.010

Friend DM, Keefe KA (2013) Glial reactivity in resistance to methamphetamine-induced neurotoxicity. J Neurochem 125:566-574. https://doi.org/10.1111/jnc.12201 [doi]

Fu L et al (2017) Therapeutic effects of anti-HMGB1 monoclonal antibody on pilocarpine-induced status epilepticus in mice. Sci Rep 7:1179. https://doi.org/10.1038/s41598-017-01325-y

Gao HM, Zhou H, Zhang F, Wilson BC, Kam W, Hong JS (2011) HMGB1 acts on microglia Mac1 to mediate chronic neuroinflammation that drives progressive neurodegeneration. J Neurosci 31:1081-1092. https://doi.org/10.1523/JNEUROSCI.3732-10.2011

Gordon CJ, Watkinson WP, O'Callaghan JP, Miller DB (1991) Effects of 3,4-methylenedioxymethamphetamine on autonomic thermoregulatory responses of the rat. Pharmacol Biochem Behav 38:339-344. https://doi.org/10.1016/0091-3057(91)90288-d

Granado N, Lastres-Becker I, Ares-Santos S, Oliva I, Martin E, Cuadrado A, Moratalla R (2011) Nrf2 deficiency potentiates methamphetamine-induced dopaminergic axonal damage and gliosis in the striatum. Glia 59:1850-1863. https://doi.org/10.1002/glia.21229

Haruma J et al (2016) Anti-high mobility group box-1 (HMGB1) antibody attenuates delayed cerebral vasospasm and brain injury after subarachnoid hemorrhage in rats. Sci Rep 6:37755. https://doi.org/10.1038/srep37755

Hozumi H et al (2008) Protective effects of interferon-γ against methamphetamine-induced neurotoxicity. Toxicol Lett 177:123-129. https://doi.org/10.1016/j.toxlet.2008.01.005

Kawasaki T, Ishihara K, Ago Y, Nakamura S, Itoh S, Baba A, Matsuda T (2006) Protective effect of the radical scavenger edaravone against methamphetamine-induced dopaminergic neurotoxicity in mouse striatum. Eur J Pharmacol 542:92-99.

https://doi.org/10.1016/j.ejphar.2006.05.012

Kays JS, Yamamoto BK (2019) Evaluation of microglia/macrophage cells from rat striatum and prefrontal cortex reveals differential expression of inflammatory-related mRNA after methamphetamine. Brain Sci 9:340. https://doi.org/10.3390/brainsci9120340

Kim JB, Lim CM, Yu YM, Lee JK (2008) Induction and subcellular localization of high-mobility group box-1 (HMGB1) in the postischemic rat brain. J Neurosci Res 86:1125-1131. https://doi.org/10.1002/jnr.21555

Kim JB et al (2006) HMGB1, a novel cytokine-like mediator linking acute neuronal death and delayed neuroinflammation in the postischemic brain. J Neurosci 26:6413-6421. https://doi.org/10.1523/JNEUROSCI.3815-05.2006

Kita T, Miyazaki I, Asanuma M, Takeshima M, Wagner GC (2009) Dopamine-induced behavioral changes and oxidative stress in methamphetamine-induced neurotoxicity. Int Rev Neurobiol 88:43-64. https://doi.org/10.1016/S0074-7742(09)88003-3

Kita T, Shimada K, Mastunari Y, Wagner GC, Kubo K, Nakashima T (2000) Methamphetamine-induced striatal dopamine neurotoxicity and cyclooxygenase-2 protein expression in BALB/c mice. Neuropharmacology 39:399-406. https://doi.org/10.1016/s0028-3908(99)00175-6

Kiyatkin EA, Brown PL, Sharma HS (2007) Brain edema and breakdown of the blood-brain barrier during methamphetamine intoxication: critical role of brain hyperthermia Eur J Neurosci 26:1242-1253. https://doi.org/10.1111/j.1460-9568.2007.05741.x

Kousik SM, Napier TC, Carvey PM (2012) The effects of psychostimulant drugs on blood brain barrier function and neuroinflammation. Front Pharmacol 3:121. https://doi.org/10.3389/fphar.2012.00121

Krasnova IN, Cadet JL (2009) Methamphetamine toxicity and messengers of death. Brain Res Rev 60:379-407. https://doi.org/10.1016/j.brainresrev.2009.03.002

Kwak MS, Kim HS, Lee B, Kim YH, Son M, Shin JS (2020) Immunological significance of HMGB1 post-translational modification and redox biology. Front Immunol 11:1189. https://doi.org/10.3389/fimmu.2020.01189

Ladenheim B et al (2000) Methamphetamine-induced neurotoxicity is attenuated in transgenic mice with a null mutation for interleukin-6. Mol Pharmacol 58:1247-1256. https://doi.org/10.1124/mol.58.6.1247

Liu K et al (2007) Anti-high mobility group box 1 monoclonal antibody ameliorates brain infarction induced by transient ischemia in rats. FASEB J 21:3904-3916. https://doi.org/10.1096/fj.07-8770com

Loftis JM, Janowsky A (2014) Neuroimmune basis of methamphetamine toxicity. Int Rev Neurobiol 118:165-197. https://doi.org/10.1016/B978-0-12-801284-0.00007-5

Mahajan SD et al (2008) Methamphetamine alters blood brain barrier permeability via the modulation of tight junction expression: Implication for HIV-1 neuropathogenesis in the context of drug abuse. Brain Res 1203:133-148. https://doi.org/10.1016/j.brainres.2008.01.093

Makisumi T, Yoshida K, Watanabe T, Tan N, Murakami N, Morimoto A (1998) Sympatho-adrenal involvement in methamphetamine-induced hyperthermia through skeletal muscle hypermetabolism. Eur J Pharmacol 363:107-112. https://doi.org/10.1016/s0014-2999(98)00758-4

Matsumoto RR, Seminerio MJ, Turner RC, Robson MJ, Nguyen L, Miller DB, O'Callaghan JP (2014) Methamphetamine-induced toxicity: an updated review on issues related to hyperthermia. Pharmacol Ther 144:28-40. https://doi.org/10.1016/j.pharmthera.2014.05.001

Miyazaki I, Asanuma M, Diaz-Corrales FJ, Fukuda M, Kitaichi K, Miyoshi K, Ogawa N (2006) Methamphetamine-induced dopaminergic neurotoxicity is regulated by quinone formation-related molecules. FASEB J 20:571-573. https://doi.org/10.1096/fj.05-4996fje

Miyazaki I, Asanuma M, Murakami S, Takeshima M, Torigoe N, Kitamura Y, Miyoshi K (2013) Targeting 5-HT1A receptors in astrocytes to protect dopaminergic neurons in parkinsonian models. Neurobiol Dis 59:244-256. https://doi.org/10.1016/j.nbd.2013.08.003

Muhammad S et al (2008) The HMGB1 receptor RAGE mediates ischemic brain damage. J Neurosci 28:12023-12031. https://doi.org/10.1523/JNEUROSCI.2435-08.2008

Nakamura Y et al (2013) Neuropathic pain in rats with a partial sciatic nerve ligation is alleviated by intravenous injection of monoclonal antibody to high mobility group box-1. PLoS One 8:e73640. https://doi.org/10.1371/journal.pone.0073640

Okuma Y et al (2012) Anti-high mobility group box-1 antibody therapy for traumatic brain injury Ann Neurol 72:373-384. https://doi.org/10.1002/ana.23602

Papageorgiou M, Raza A, Fraser S, Nurgali K, Apostolopoulos V (2019) Methamphetamine and its immune-modulating effects. Maturitas 121:13-21. https://doi.org/10.1016/j.maturitas.2018.12.003

Park JS, Svetkauskaite D, He Q, Kim JY, Strassheim D, Ishizaka A, Abraham E (2004) Involvement of toll-like receptors 2 and 4 in cellular activation by high mobility

group box 1 protein. J Biol Chem 279:7370-7377. https://doi.org/10.1074/jbc.M306793200

Paudel YN et al (2018) HMGB1: A Common Biomarker and Potential Target for TBI, Neuroinflammation, Epilepsy, and Cognitive Dysfunction. Front Neurosci 12:628. https://doi.org/10.3389/fnins.2018.00628

Qiu J et al (2008) Early release of HMGB-1 from neurons after the onset of brain ischemia. J Cereb Blood Flow Metab 28:927-938. https://doi.org/10.1038/sj.jcbfm.9600582

Raineri M et al (2012) Modafinil abrogates methamphetamine-induced neuroinflammation and apoptotic effects in the mouse striatum. PLoS One 7:e46599. https://doi.org/10.1371/journal.pone.0046599

Sasaki T et al (2016) Anti-high mobility group box 1 antibody exerts neuroprotection in a rat model of Parkinson's disease. Exp Neurol 275 Pt 1:220-231. https://doi.org/10.1016/j.expneurol.2015.11.003

Seminerio MJ, Robson MJ, McCurdy CR, Matsumoto RR (2012) Sigma receptor antagonists attenuate acute methamphetamine-induced hyperthermia by a mechanism independent of IL-1β mRNA expression in the hypothalamus. Eur J Pharmacol 691:103-109. https://doi.org/10.1016/j.ejphar.2012.07.029

Shi Y, Zhang L, Teng J, Miao W (2018) HMGB1 mediates microglia activation via the TLR4/NF-κB pathway in coriaria lactone induced epilepsy. Mol Med Rep 17:5125-5131. https://doi.org/10.3892/mmr.2018.8485

Shibasaki M et al (2010) Induction of high mobility group box-1 in dorsal root ganglion contributes to pain hypersensitivity after peripheral nerve injury. Pain 149:514-521. https://doi.org/10.1016/j.pain.2010.03.023

Tang D, Kang R, Zeh HJ III, Lotze MT (2011) High-mobility group box 1, oxidative stress, and disease. Antioxid Redox Signal 14:1315-1335. https://doi.org/10.1089/ars.2010.3356

Thomas DM, Kuhn DM (2005) Attenuated microglial activation mediates tolerance to the neurotoxic effects of methamphetamine. J Neurochem 92:790-797. https://doi.org/10.1111/j.1471-4159.2004.02906.x

Thomas DM, Walker PD, Benjamins JA, Geddes TJ, Kuhn DM (2004) Methamphetamine neurotoxicity in dopamine nerve endings of the striatum is associated with microglial activation. J Pharmacol Exp Ther 311:1-7. https://doi.org/10.1124/jpet.104.070961

Thrash-Williams B, Karuppagounder SS, Bhattacharya D, Ahuja M, Suppiramaniam V, Dhanasekaran M (2016) Methamphetamine-induced dopaminergic toxicity prevented

owing to the neuroprotective effects of salicylic acid. Life Sci 154:24-29. https://doi.org/10.1016/j.lfs.2016.02.072

Tsuji T, Asanuma M, Miyazaki I, Miyoshi K, Ogawa N (2009) Reduction of nuclear peroxisome proliferator-activated receptor gamma expression in methamphetamine-induced neurotoxicity and neuroprotective effects of ibuprofen. Neurochem Res 34:764-774. https://doi.org/10.1007/s11064-008-9863-x

Vargas AM, Rivera-Rodriguez DE, Martinez LR (2020) Methamphetamine alters the TLR4 signaling pathway, NF-kB activation, and pro-inflammatory cytokine production in LPS-challenged NR-9460 microglia-like cells. Mol Immunol 121:159-166. https://doi.org/10.1016/j.molimm.2020.03.013

Wang D, Liu K, Wake H, Teshigawara K, Mori S, Nishibori M (2017) Anti-high mobility group box-1 (HMGB1) antibody inhibits hemorrhage-induced brain injury and improved neurological deficits in rats. Sci Rep 7:46243. https://doi.org/10.1038/srep46243

Yamaguchi T, Kuraishi Y, Minami M, Nakai S, Hirai Y, Satoh M (1991) Methamphetamine-induced expression of interleukin-1β mRNA in the rat hypothalamus. Neurosci Lett 128:90-92. https://doi.org/10.1016/0304-3940(91)90766-m

Zhang FF et al (2016) Perineural expression of high-mobility group box-1 contributes to long-lasting mechanical hypersensitivity via matrix metalloprotease-9 up-regulation in mice with painful peripheral neuropathy. J Neurochem 136:837-850. https://doi.org/10.1111/jnc.13434

Zhang J et al (2011) Anti-high mobility group box-1 monoclonal antibody protects the blood-brain barrier from ischemia-induced disruption in rats. Stroke 42:1420-1428. https://doi.org/10.1161/STROKEAHA.110.598334

Zhang L, Kitaichi K, Fujimoto Y, Nakayama H, Shimizu E, Iyo M, Hashimoto K (2006) Protective effects of minocycline on behavioral changes and neurotoxicity in mice after administration of methamphetamine. Prog Neuropsychopharmacol Biol Psychiatry 30:1381-1393. https://doi.org/10.1016/j.pnpbp.2006.05.015

Zhang Y, Zhu T, Zhang X, Chao J, Hu G, Yao H (2015) Role of high-mobility group box 1 in methamphetamine-induced activation and migration of astrocytes. J Neuroinflammation 12:156. https://doi.org/10.1186/s12974-015-0374-9

Figure legends

Fig. 1. Effects of anti-HMGB1 mAb injection on METH-induced hyperthermia and changes in plasma HMGB1 concentration. **A:** Schematic illustration of the experimental protocol. BALB/c mice received intravenous administration of anti-HMGB1 mAb (1 mg/kg), class-matched control IgG, or PBS, followed by METH (4 mg/kg ×2, i.p. with 2-h interval). Rectal temperature (♦) was recorded just before or every 1 h after the first METH injection for up to 5 h. Striatal nuclear protein was extracted 2 h after the second METH injection. Plasma was collected 6 h after the first METH injection. Three days after the METH injections, mice were transcardially perfused with saline followed by a fixative, and brains were obtained. **B:** Rectal temperature was recorded every 1 h after the first METH injection. *$p < 0.01$ vs. each preinjection. #$p < 0.01$, ##$p < 0.001$ vs. time-matched saline + PBS-treated group. \$$p < 0.01$ vs. time-matched METH + PBS-treated group. (two-way ANOVA) **C:** Plasma HMGB1 concentration 6 h after the last injection of METH or saline. Each value represents the mean ± SEM, saline + PBS (n = 5), saline + IgG (n = 4), saline + HMGB1 Ab (n = 4), METH + PBS (n = 6), METH + IgG (n = 6), METH + HMGB1 Ab (n = 6). *$p < 0.05$, **$p < 0.01$ vs. saline + PBS-treated group. ##$p < 0.01$ vs. saline + IgG-treated group. \$$p < 0.05$ vs. METH + IgG-treated group. (one-way ANOVA followed by Fisher's PLSD test)

Fig. 2. Effects of anti-HMGB mAb injection on METH-induced degeneration of dopaminergic nerve terminals. **A:** Representative photomicrographs of immunohistochemical staining of DAT in the mouse mid-striatum three days after the last METH injection (4 mg/kg ×2, i.p. with 2 h interval). Scale bar = 500 μm. **B:** Quantitative data of DAT-immunoreactive signal intensity. Each value represents the mean ± SEM, saline + PBS (n = 4), saline + IgG (n = 4), saline + HMGB1 Ab (n = 4), METH + PBS (n = 5), METH + IgG (n = 6), METH + HMGB1 Ab (n = 4). **$p < 0.01$, ***$p < 0.001$ vs. saline + PBS-treated group. ###$p < 0.001$ between indicated two groups. (one-way ANOVA followed by Fisher's PLSD test)

Fig. 3. Effects of anti-HMGB1 mAb injection on METH-induced accumulation of Iba1-positive microglial cells in the mouse mid-striatum. **A:** Representative photomicrographs of immunohistochemical staining of Iba1 in the central part of mid-striatum three days after the METH injection. Scale bar = 100 μm. **B:** Magnified photographs of Iba1 immunostaining. Scale bar = 100 μm. **C:** Quantitative data of the number of Iba1-positive cells. Each value represents the mean ± SEM, saline + PBS (n = 4),

saline + IgG (n = 4), saline + HMGB1 Ab (n = 4), METH + PBS (n = 5), METH + IgG (n = 6), METH + HMGB1 Ab (n = 4). *$p < 0.05$, ***$p < 0.001$ vs. saline + PBS-treated group. #$p < 0.05$, ##$p < 0.01$ between indicated two groups. (one-way ANOVA followed by Fisher's PLSD test)

Fig. 4. Effects of anti-HMGB1 mAb injection on METH-induced BBB disruption. **A:** Representative photomicrographs of immunohistochemical staining of albumin in the striatum of mice three days after the METH injection. Scale bar = 500 μm. **B:** Quantitative data of albumin-immunoreactive signal intensity. Each value is the mean ± SEM, saline + PBS (n = 4), saline + IgG (n = 4), saline + HMGB1 Ab (n = 4), METH + PBS (n = 5), METH + IgG (n = 5), METH + HMGB1 Ab (n = 5). *$p < 0.05$, **$p < 0.01$ vs. saline + PBS-treated group. (one-way ANOVA followed by Fisher's PLSD test)

Fig. 5. Effects of METH and anti-HMGB1 mAb on HMGB1 translocation in the striatal neuronal cells. Representative photomicrographs of HMGB1 and NeuN double immunostaining in the mouse mid-striatum three days after the METH injection. Green: HMGB1. Red: NeuN. Blue: Hoechst 33342. The arrowhead shows HMGB1 released from the nuclei. Scale bar = 20 μm.

Fig. 6. HMGB1 expression in the striatal astrocytes. Representative photomicrographs of HMGB1 and GS double immunostaining in the mouse mid-striatum three days after the METH injection. Green: HMGB1. Red: GS. Blue: Hoechst 33342. Scale bar = 20 μm.

Fig. 1

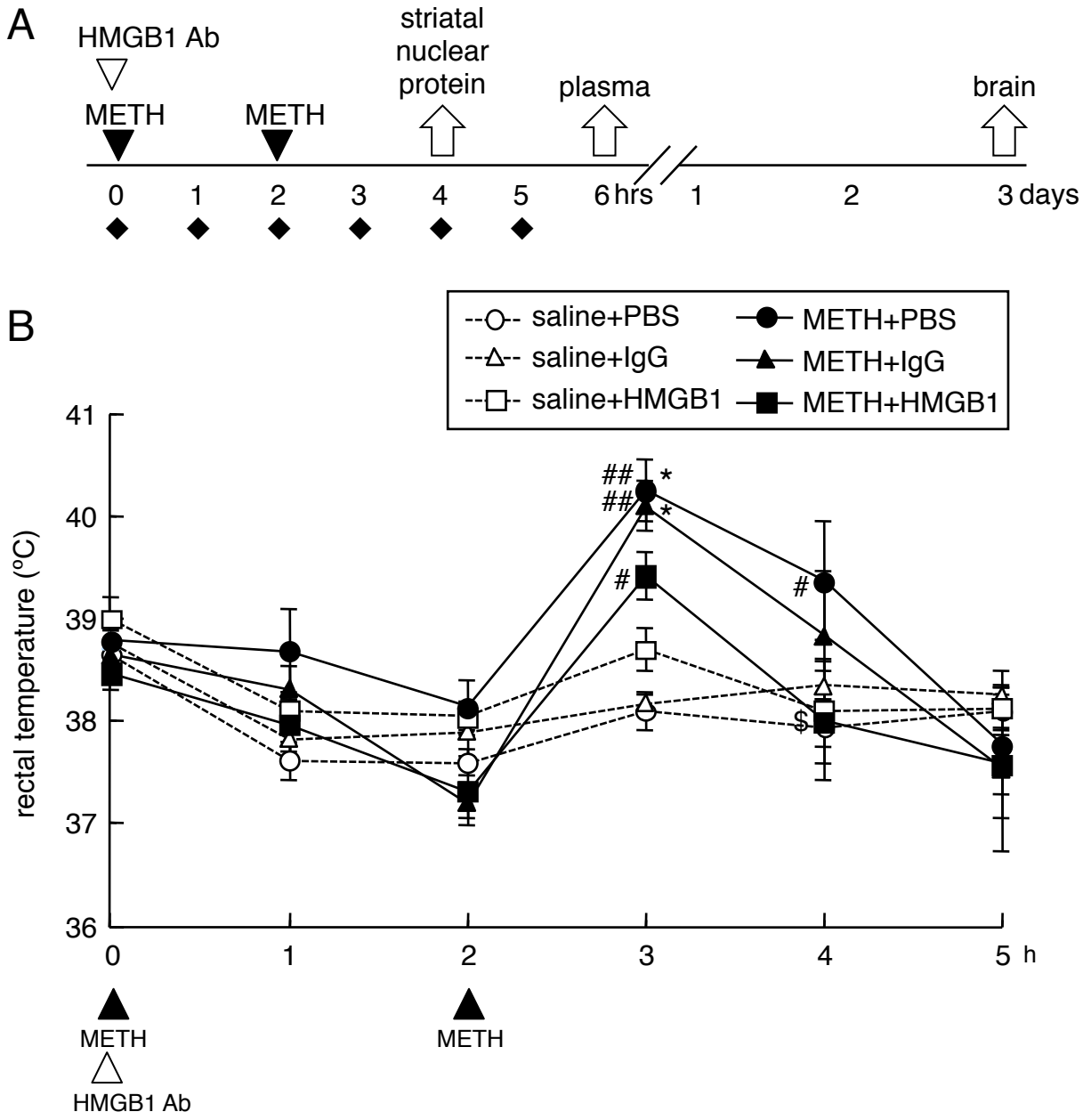
A
HMGB1 Ab
METH
METH
striatal nuclear protein
plasma
brain
0 1 2 3 4 5 6 hrs 1 2 3 days
B
saline+PBS
saline+IgG
saline+HMGB1
METH+PBS
METH+IgG
METH+HMGB1
rectal temperature (°C)
41
40
39
38
37
36
0 1 2 3 4 5 h
METH
METH
HMGB1 Ab
C
concentration of plasma HMGB1 (ng/ml)
50
40
30
20
10
0
PBS IgG HMGB1 Ab PBS IgG HMGB1 Ab
saline
METH

Fig. 2

A

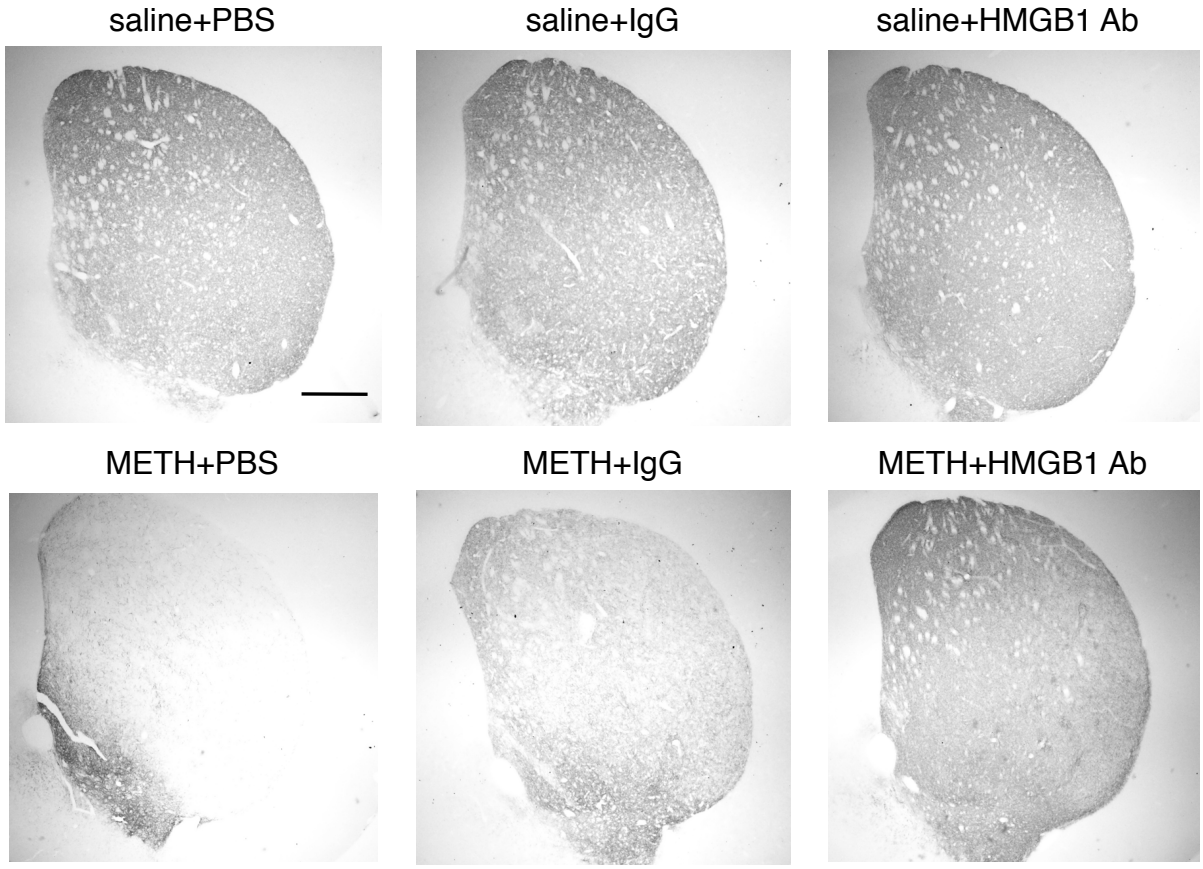
saline+PBS
saline+IgG
saline+HMGB1 Ab
METH+PBS
METH+IgG
METH+HMGB1 Ab

B

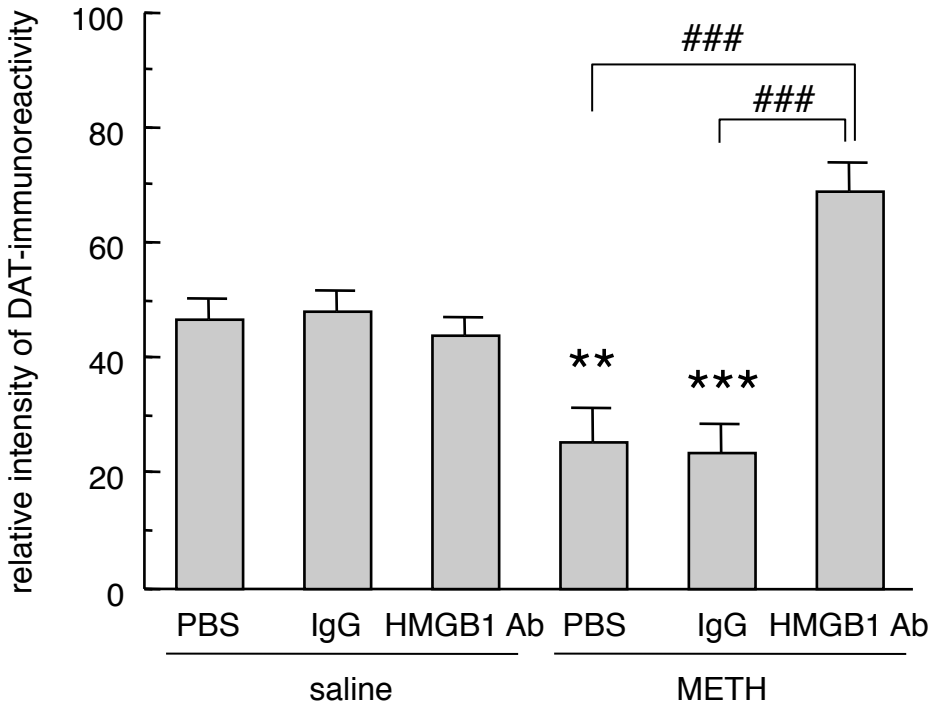
relative intensity of DAT-immunoreactivity
100
80
60
40
20
0
###
###
**
***
PBS
IgG
HMGB1 Ab
PBS
IgG
HMGB1 Ab
saline
METH

Fig. 3

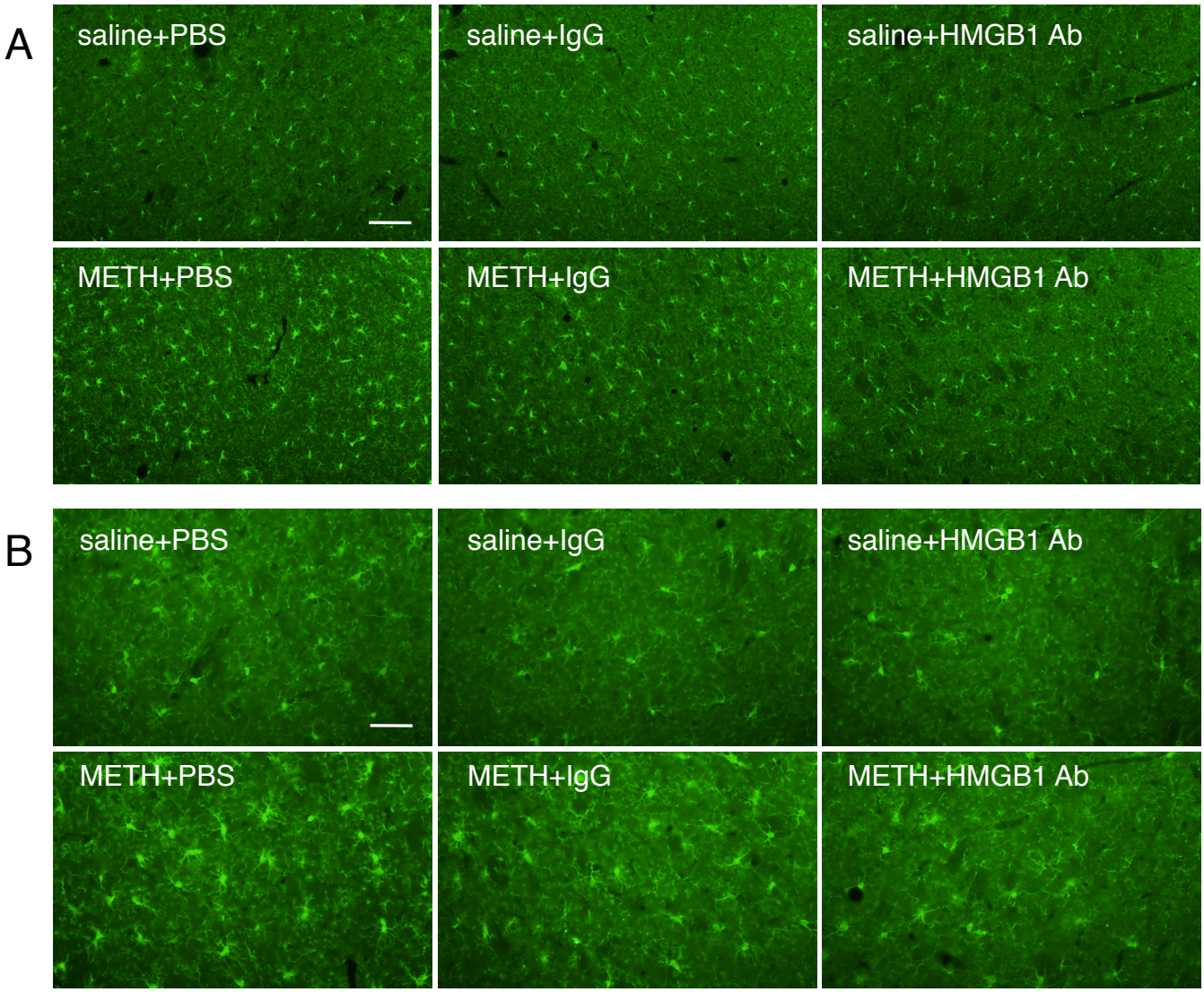
A
saline+PBS
saline+IgG
saline+HMGB1 Ab
METH+PBS
METH+IgG
METH+HMGB1 Ab
B
saline+PBS
saline+IgG
saline+HMGB1 Ab
METH+PBS
METH+IgG
METH+HMGB1 Ab

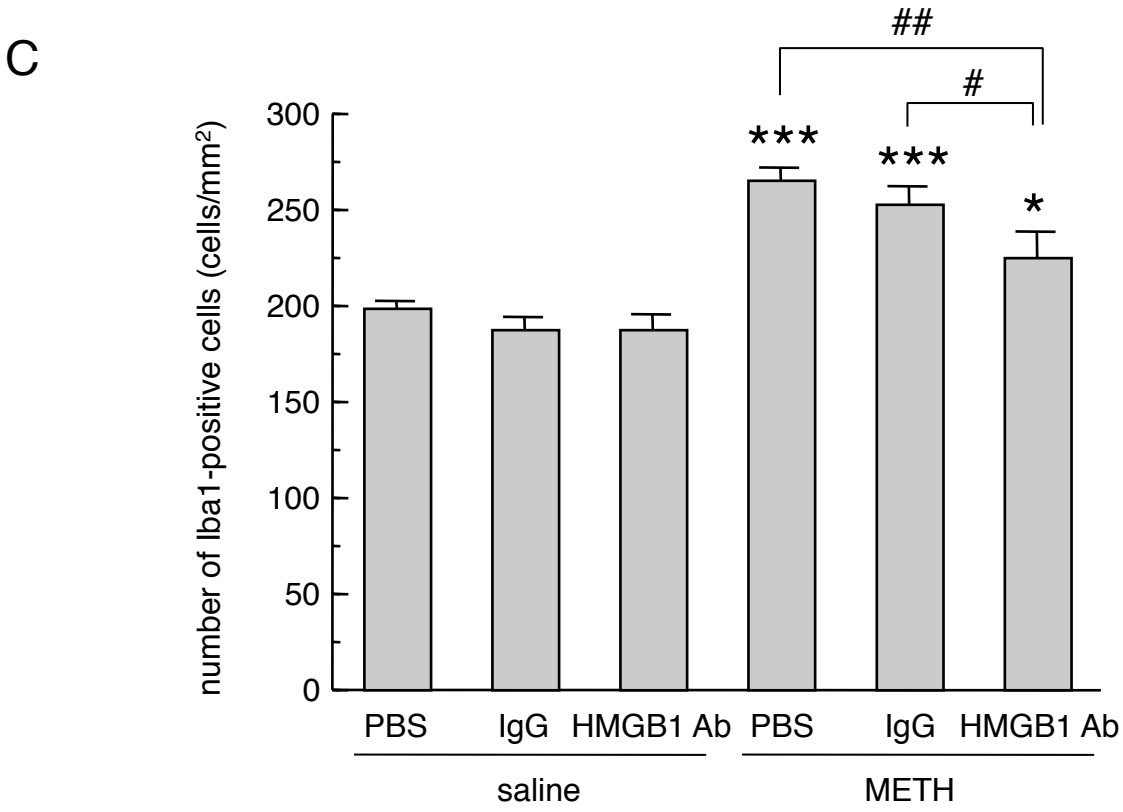
C
##
#
***
***
*
number of Iba1-positive cells (cells/mm²)
300
250
200
150
100
50
0
PBS
IgG
HMGB1 Ab
PBS
IgG
HMGB1 Ab
saline
METH

Fig. 4

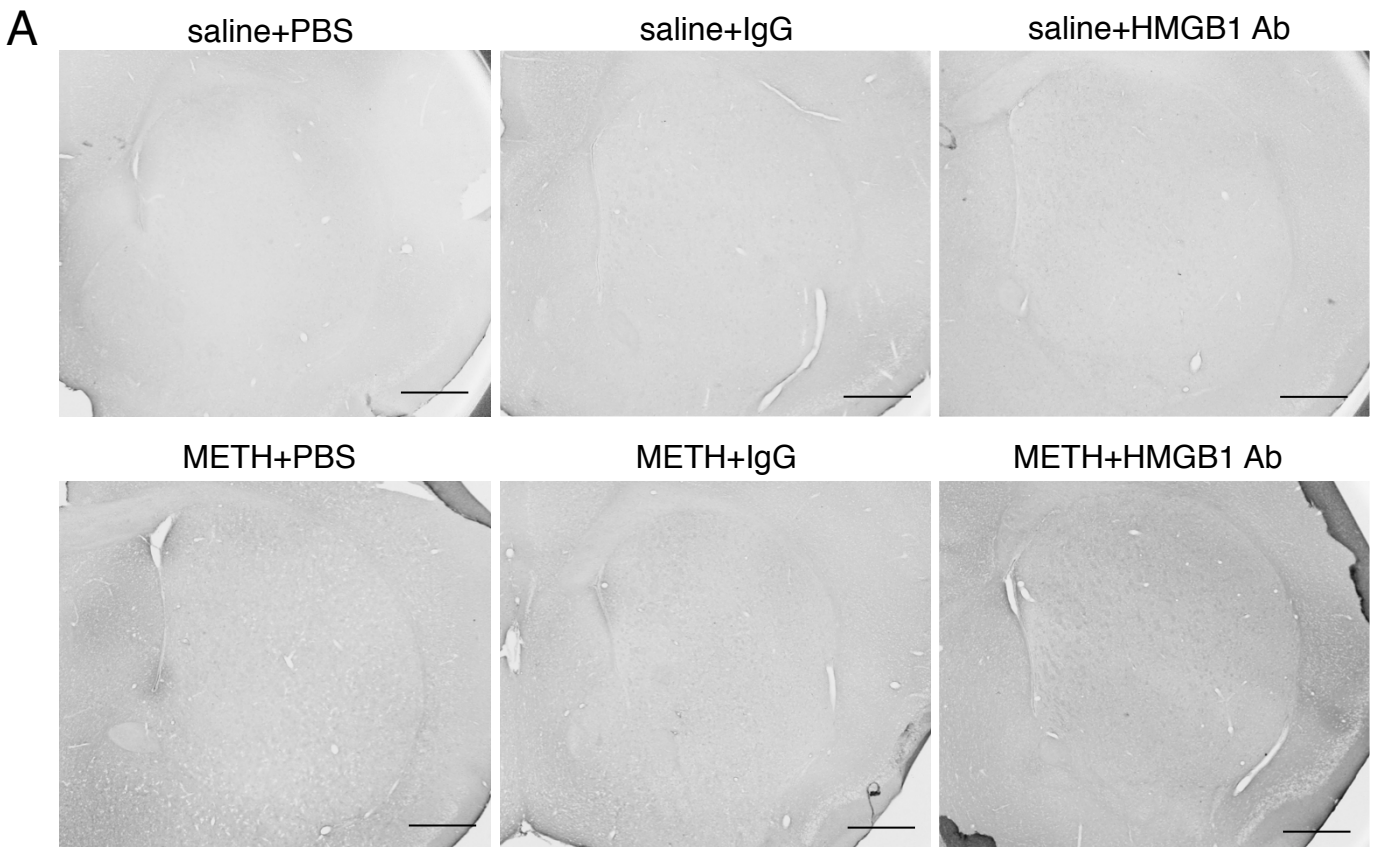
A
saline+PBS
saline+IgG
saline+HMGB1 Ab
METH+PBS
METH+IgG
METH+HMGB1 Ab

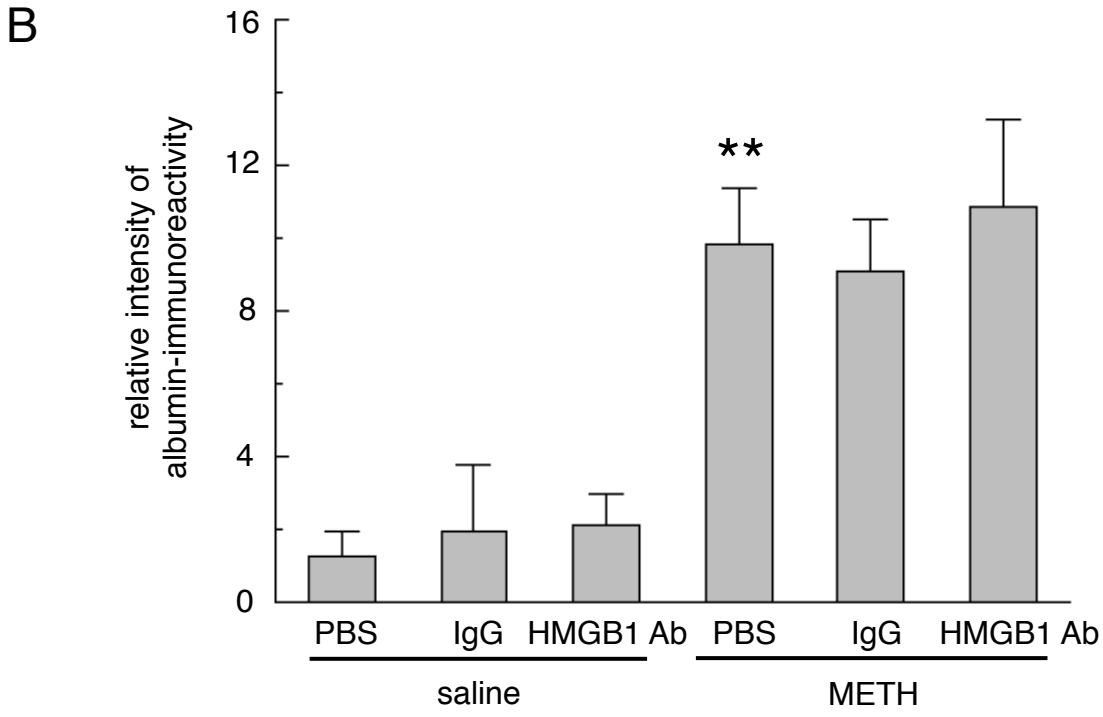
B
relative intensity of albumin-immunoreactivity
16
12
8
4
0
**
PBS
IgG
HMGB1 Ab
PBS
IgG
HMGB1 Ab
saline
METH

Fig. 5

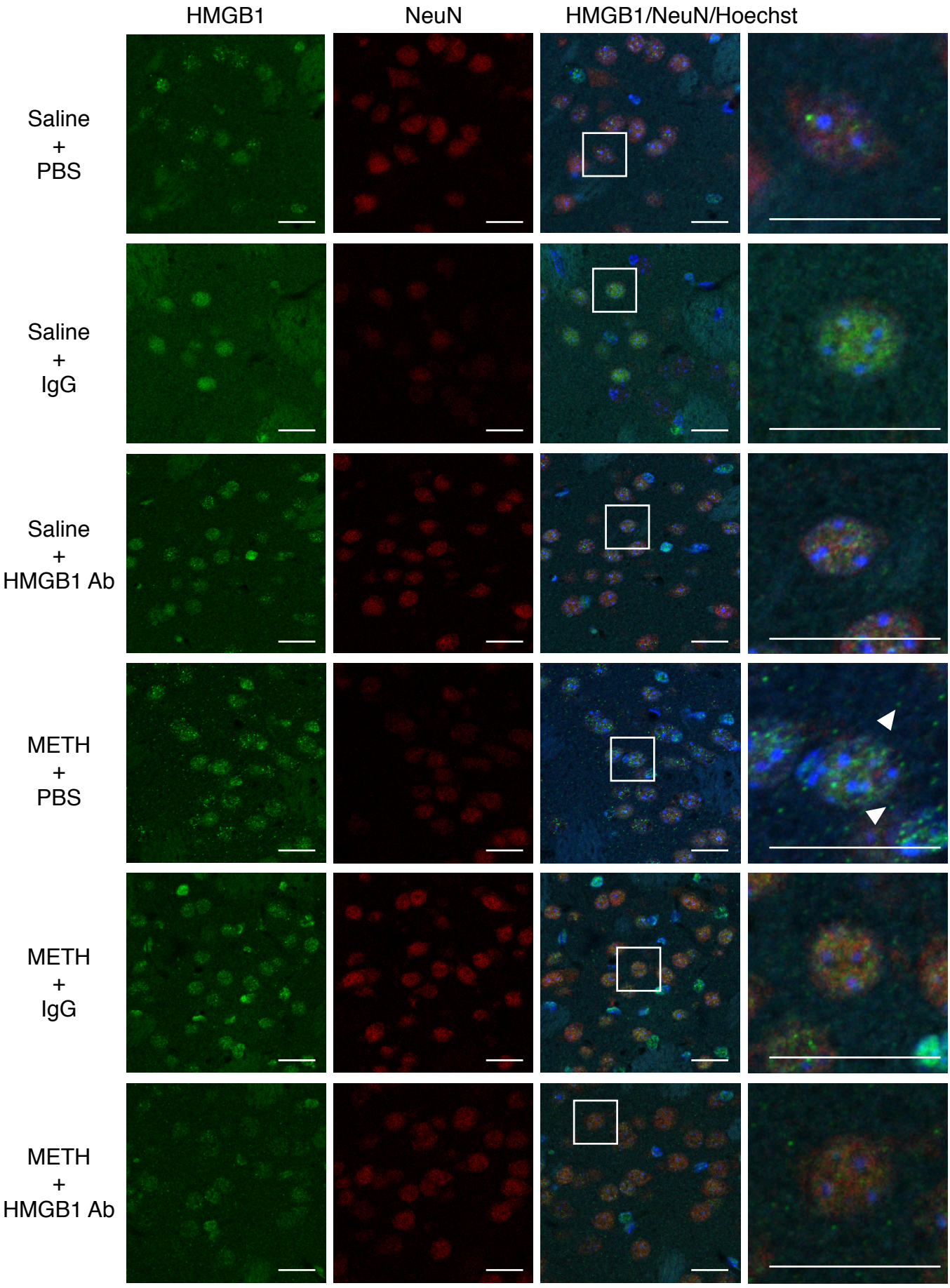
HMGB1
NeuN
HMGB1/NeuN/Hoechst
Saline + PBS
Saline + IgG
Saline + HMGB1 Ab
METH + PBS
METH + IgG
METH + HMGB1 Ab

Fig. 6

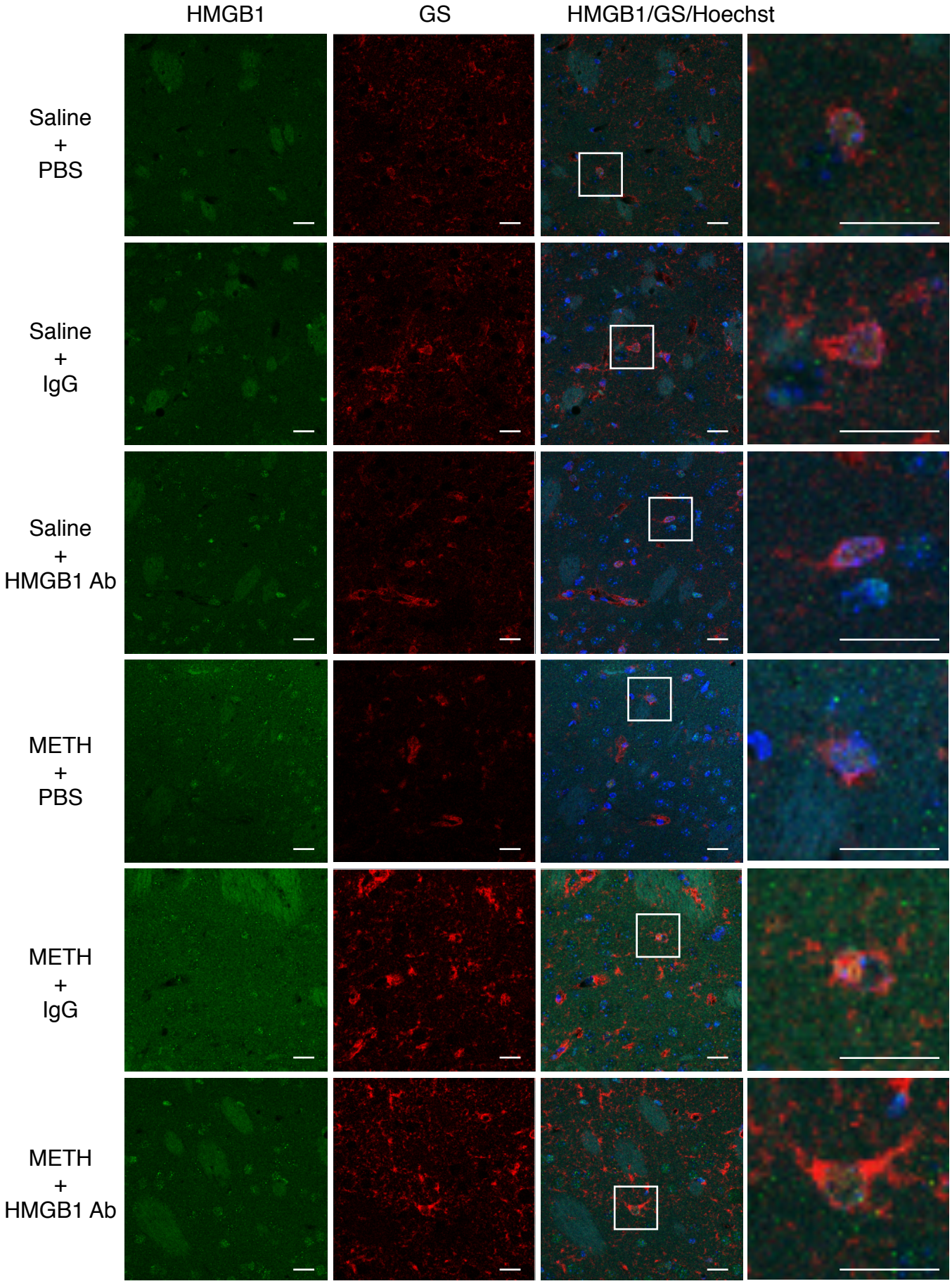
HMGB1
GS
HMGB1/GS/Hoechst
Saline + PBS
Saline + IgG
Saline + HMGB1 Ab
METH + PBS
METH + IgG
METH + HMGB1 Ab